Received: 25 February 2024 | Revised: 17 April 2024 | Accepted: 20 May 2024

DOI: 10.1002/pol.20240152

RESEARCH ARTICLE

JOURNAL OF POLYMER SCIENCE WILEY

Shaping the structure and properties of HyTemp using polyethylene glycol diglycidyl ether cross-linkers

Eleftheria Dossi[1] | **Khuthadzo Lourate Mutele-Nkuna**[2] | **Peter Wilkinson**[1] | **Guillaume Kister**[1] | **Hugh Patrick**[3] | **Mohammad Hakim Khalili**[4] | **Sara Hawi**[4]

[1]Centre for Defence Chemistry, Cranfield University, Defence Academy of the United Kingdom, Shrivenham, UK

[2]SO 1 Technical, System Naval Ordnance, Fleet Command Headquarters, Western Cape, South Africa

[3]Defence Science and Technology Laboratory, Salisbury, Wiltshire, UK

[4]Surface Engineering and Precision Centre, School of Aerospace, Transport and Manufacturing, Cranfield University, Wharley End, UK

Correspondence
Eleftheria Dossi, Centre for Defence Chemistry, Cranfield University, Defence Academy of the United Kingdom, Shrivenham SN6 8LA, UK.
Email: e.dossi@cranfield.ac.uk

Funding information
Cranfield University

Abstract

Novel elastomers are made by reaction of hydroxyl-terminated polyacrylic ester (HyTemp) with polyethylene glycol (PEG, number of ethylene glycol units 1, 3, 6, 9) based cross-linkers. The influence of the cross-linker length, the HyTemp/cross-linker (w/w) ratio and the cross-linking accelerator trifluoromethanesulfonate scandium salt (ScTFMS) on the structure and the properties of the materials are studied. The cross-linker length has not influence on the glass transition (T_g) of the products because of the presence of the flexible PEG units that cancels out the cross-linking effect associated to a shift to higher T_g. A two-domain structure is seen by the presence of a dual T_g in samples cured with ScTFMS. Mathematical analysis of the modulated differential scanning calorimetry curves offers for the first time the possibility to identify/confirm structural differences in complex three-dimensional polymeric structures. Scanning electron microscopy and swelling experiments in ethyl acetate respectively reveal an increase in the pore size (1.13 to 5.48 nm) and in the absorption ability of the elastomers cured with different types and quantities of PEG cross-linker. The new elastomeric materials are exhibiting a rubbery state over a wide temperature range and absorptivity for the potential recovery of pollutants in soil and/or water.

KEYWORDS

curing, diglycidyl ethers, elastomer, modulated differential scanning calorimetry, swelling

1 | INTRODUCTION

Macromolecular engineering has assisted on the development of new polymeric materials for an extensive range of applications.[1–3] The design and synthesis of polymers can be directed to very specific areas due to the material's properties, such as diversity of molecular architectures, dimensional stability, mechanical orientability, durability, ease of processability, malleability, and smart response to external stimuli.[4–6] Among the main polymeric classes, elastomers are characterized by high flexibility, durability, and reliability.[7] They are often amorphous polymers with a glass transition temperature (reversible glassy to rubbery state transition) far below room temperature.[5] Cross-linking

through sulfur vulcanization or peroxide curing[8,9] for example, can influence the elastic behavior of long-chain molecules by creating cross-linking points forming three-dimensional (3D) networks. The resulting elastomers exhibit different thermal and mechanical properties depending on the chemical structure of both polymer matrix and cross-linker, on their ratio and on the curing reaction conditions. A variety of cross-linkers containing two or more reactive (functional) groups, such as isocyanates, epoxides, carboxylic acids, and amines can be used.[10] Isocyanates are the most common cross-linkers for manufacturing elastomeric polyurethanes however their use is becoming more restricted due to tighter safety regulations related to their production and toxicity.[11] A viable alternative to isocyanates are nontoxic cross-linkers, such as diepoxides used in the production of polyether elastomers from polyols.[12,13] The cross-linking density and the bulk properties of the 3D structures are also affected by the use of cross-linking accelerators, small molecules that can help initiate and accelerate the cross-linking process.[14] The accelerators can be organic salts of metals, such as scandium or yttrium. For example, their triflate salts provide increased rates of reaction and are more cost effective.[12]

Among their excellent viscoelastic properties, elastomers often show a very good ability to swell by absorbing water or organic solvents within their structure.[15] The swelling is due to the solvent penetration into the void space between the polymeric chain networks, which can be influenced by external triggers such as pH, ionic strength, and temperature. The chemical structure of both polymer and cross-linker also influences the swelling characteristics[16–19] and the potential applications of elastomers.[8,20,21] For example, poly methyl methacrylate (PMMA) or poly(ethylene glycol) diacrylate (PEGDA) can be transformed into hydrogels through cross-linking, producing substrates for biomedical applications including tissue engineering and regenerative medicine, drug delivery, cancer therapies and biosensing.[22–25] Polyacrylamide homopolymers (PAAm) and PAAm copolymers with methyl methacrylate monomer (MMA) formed hydrogels with a variety of properties, such as better mechanical properties or better biocompatibility and swelling when compared with their basic polymer structures.[26] The copolymerisation of PAAm with MMA produced hydrogels with different swelling behaviors controlled by the porosity of the polymeric material.

HyTemp 4454, a hydroxyl-terminated polyacrylate copolymer chosen in this research, is made by the copolymerisation of ethyl acrylate, butyl acrylate, methacrylic acid, and vinyl chloroacetate and contains a small percentage of chlorine and carboxyl cross-linkable sites as pendant groups of the backbone.[13,27,28] HyTemp shows excellent heat and processing properties and excellent low-temperature performance when vulcanized with peroxide.[27] HyTemp is soluble in chloroform and ethyl acetate and is reported to cure with a variety of non-isocyanate cross-linkers, among them quaternary ammonium compounds (halides).[18,29,30] When triethylene glycol diglycidyl ether was used by the authors of this article, two glass transitions were observed for the cross-linked HyTemp 4454 structures, which was attributed to two distinct regions with dissimilar thermal behavior.[13] Metal salts such as trifluoromethanesulfonates are also used as catalysts to accelerate the curing and to achieve a high degree of cross-linking.[31] Limited information about modification processes of HyTemp is available in the public domain because of restricted access to technical meetings or Patents. Diamine cross-linking agents used in a composition of the 1,8 -diazabicyclo [5,4,0] undec -7-ene accelerator, a pyrrolidone type activator and a secondary or tertiary aliphatic amine are reported achieving similar mechanical properties to HyTemp cured with guanidine based cross-linking agent.[32] Metal fatty acid salts (stearate or oleate) are used as curatives in Zeon products[33] and to promote the cross-linking of mixtures of polyamide or polyester with acrylate rubbers having dissimilar functional groups.[34]

N,N′-di-o-tolylguanidine (DOTG) also reported as a curative for HyTemp polyacrylate elastomers but currently is under US and EU REACH regulatory concerns. Guanidine-free cured systems that maintain high performance are highly desirable as alternatives to DOTG.[35]

The authors have used REACH compliant polyethylene glycol diglycidyl ethers having three or more ethylene groups in the chain in the cross-linking of synthetic and natural precursors;[36] it is expected to influence the chemico-physical, thermal, and mechanical properties of HyTemp and have a high potential on replacing current cross-linkers. In this context, the aim of this project was to study, the influence of the length and amount of polyethylene glycol (PEG)-based cross-linking spacers on the properties of cured HyTemp 4454. To achieve this, we selected four diglycidyl ethers, namely ethylene glycol (EGDGE, 1xPEG unit), triethylene glycol (TEGDGE, 3xPEG units), hexaethylene glycol (HEGDGE, 6xPEG units) and polyethylene glycol (PEGDGE, 9xPEG units). This is the first time in the literature that EGDGE, HEGDGE, and PEGDGE cross-linkers are used in the curing of HyTemp. Diepoxyoctane was also used to check the influence of the oxygen atoms on the cross-linker spacer and consequently on the properties of the cured system. Trifluoromethanesulfonate scandium salt (ScTFMS) was used in selected samples to accelerate the curing process. We found that we can control by design the bulk and thermal properties of the elastomeric

materials and consequently their performance and applications. The only dual glass transitions observed by thermal analysis are characteristic of some block copolymers,[37] further investigation is in progress for linking this unique property to the materials and their potential applications. The important swelling ability of the synthesized cross-linked materials makes them suitable as potential nontoxic adjuvants[38] for the recovery of pollutants in soil or water.

2 | EXPERIMENTAL SECTION

2.1 | Materials and characterization methods

EDGDE (CAS Number 2224-15-9) and PEGDGE (CAS Number 26403-72-5, M_n 500) were purchased from Tokyo Chemical Industry and Sigma-Aldrich respectively. TEGDGE (99.8% by ^{1}H NMR, Figure S1) and HEGDGE (99.8% by ^{1}H NMR, Figure S2) were synthesized at Cranfield University according to procedures described.[13,39] HyTemp 4454 (ZEON Chemicals, Figures S3–S5) was kindly provided by AWE UK. ScTFMS (CAS Number 144026-79-9) was purchased by Fluka. All other reagents and solvents were used as received from Sigma-Aldrich. The chemical structure of soluble samples (typically 20 mg/mL) was analyzed by Proton Nuclear Magnetic Resonance (^{1}H NMR) on a Bruker Ascend 400 MHz spectrometer with a double resonance broad band probe, BBFO model, in deuterated chloroform ($CDCl_3$) or acetone-d_6 solution (Goss Scientific, >99.0%). Tetramethylsilane (TMS, Goss Scientific) used as an internal reference while peak multiplicities are described in the following way: multiplet (m).

Thermal analysis was performed on a Mettler Toledo DSC3+ instrument and analyzed using STARe version 15.00 software. A 10–15 mg of the material was placed in a Mettler Toledo 40 μL aluminum pan with a pierced lid, with a nitrogen purge of 50 mL min^{-1}. Samples were cycled two times between −100 and 30°C at 10°C min^{-1} heating/cooling rate, with the second cycle being analyzed. MDSC was conducted using Mettler Toledo's multifrequency modulated DSC, TOPEM. MDSC experiments were performed in the same manner as the regular DSC experiment, except that only one cycle from −90 to 0°C was conducted. This had an average heating rate of 2°C min^{-1}, pulse height of ±0.5°C and pulse width of 15–30 s. Evaluation used a calculation window of 120 s, window shift of 10 s and smoothing window of 90 s.

Dynamic mechanical analysis (DMA) was done by means of a Perkin Elmer DMA 8000 at oscillating frequency of 1, 5, and 10 Hz using the single cantilever configuration. Approximately 0.05 g of cured samples was folded into rectangular aluminum pockets (dimensions of 7.5 mm × 18 mm) because of the difficulty in casting DMA bars with good integrity. The samples were cooled down to −130°C using liquid nitrogen and held isothermally for 5 min before increasing the temperature up to 60°C at a heating rate of 5°C min^{-1}. One single sample of each composition was analyzed by DMA.

The surface and interior morphology of selected samples were analyzed by using Scanning Electron Microsope Hitachi SU3500 instrument at an acceleration voltage of 20 kV at 80 Pa and Scanning Electron Microscope (VEGA3, TESCAN) at an acceleration voltage of 10 kV and 3 nA beam current. For surface analysis, a small section of each sample was cut with a knife and imaged. The same samples were then freeze-dried to remove water and a section was cut for imaging. For interior morphology analysis, samples were prepared using freeze-drying method to remove water and consequently coated prior to imaging with 20 nm gold film using sputter coater. The backscattered images were captured at 1, 10, and 20 k magnifications. Swelled samples were also analyzed; samples were prepared by equilibrated in deionized water at 25°C for 48 h. The swelled samples stored in the fridge to reduce the temperature gradually to 5–7°C, then in standard freezer to reduce temperature to −28°C and finally stored in deep freezer at −60°C for 24 h. The samples loaded in the freeze-drier and stored for 4 days, then were cut with stainless steel blade (100 μm thick) and a cross-section of samples were attached to SEM stud and gold-coated with 10 nm gold before imaging.

The swelling properties of all cured materials were studied using dried solid samples (20–30 mg) immersed in ethyl acetate (for 2 h) and distilled water for the Scanning Electron Microsopy (SEM) experiments (for 48 h) under stirring (100 rpm) at ambient. The amount of solvent was sufficient for the entire sample to be completely submerged in it. The swelled gels were then removed from the solvent and the swelling degree (SD) was calculated using Equation (1).

$$\mathrm{SD} = \frac{\text{Swelled sample (g)} - \text{dry sample (g)}}{\text{Dry sample (g)}} \times 100. \quad (1)$$

2.2 | Curing procedure

HyTemp samples (0.5 g) were dissolved in 25 mL of ethyl acetate, the cross-linker (1.00, 0.75, 0.50, and 0.25 w/w)

was added to the solution and magnetically stirred for 10 min to promote homogeneous mixing (Batches A, B, C, and D, respectively). ScTFMS (2% w/w) was added to selected samples (Batch E) while stirred for further 10 min. The solvent was evaporated, and the samples were placed in a thermostatically controlled oven at 70°C for up to 20 days. A small aliquot of the reaction mixture was taken and analyzed by ^{1}H NMR spectroscopy on times 0, 4, 8, and 12 days. After curing the samples from batches A to D were purified from excess of cross-linker by extraction with hot acetone (Soxhlet). All cured products were dried and characterized by DSC, MDSC, DMA, SEM, and swelling measurements.

3 | RESULTS AND DISCUSSION

Four batches (A–D) of cross-linked HyTemp samples were produced by using variable amounts (HyTemp: cross-linker = 3.5:1.00, 3.5:0.75, 3.5:0.50, and 3.5:0.25 w/w) of five cross-linkers EGDGE, TEGDGE, HEGDGE, PEGDGE, and DEO (Table 1). A fifth batch (E) was made by using the same amounts of the five cross-linkers and with an additional amount (2% w/w) of ScTFMS to accelerate the curing process under the same experimental conditions (70°C) and observe for any structural differences in the cross-linked HyTemp samples.

The curing progress of all the samples was monitored at regular intervals of 4, 8, 12, and 20 days

TABLE 1 Synthesis and properties of cured HyTemp samples starting from 3.5 g of HyTemp.

Sample	Cross-linker	Batch[a]	Mass of cross-linker[b]	T_g by DSC (°C)[c]	T_g by DMA (°C)[d]
CHTE-A	EGDGE	A	1.00	−36.4	−31.9
CHTE-B		B	0.75	−36.7	−31.7
CHTE-C		C	0.50	−38.1	−30.9
CHTE-D		D	0.25	−37.6	Not tested[e]
CHTE-E		E	1.00[f]	−38.9 and −10.8	−33.9
CHTT-A	TEGDGE	A	1.00	−38.7	−31.8
CHTT-B		B	0.75	−38.1	−30.9
CHTT-C		C	0.50	−37.2	−31.7
CHTT-D		D	0.25	−37.6	Not tested[e]
CHTT-E		E	1.00[f]	−39.2[g]	−33.8
CHTH-A	HEGDGE	A	1.00	−39.0	−31.0
CHTH-B		B	0.75	−38.1	−32.4
CHTH-C		C	0.50	−38.1	−32.6
CHTH-D		D	0.25	−37.6	Not tested[e]
CHTH-E		E	1.00[f]	−45.2 and −38.4	−32.7
CHTP-A	PEGDGE	A	1.00	−39.2	−30.3
CHTP-B		B	0.75	−38.4	−29.8
CHTP-C		C	0.50	−37.9	−32.0
CHTP-D		D	0.25	−37.8	Not tested[e]
CHTP-E		E	1.00[f]	−47.4 and −39.2	−34.0
CHTD-A	DEO	A	1.00	−37.4	−31.4
CHTD-B		B	0.75	−37.6	−30.1
CHTD-C		C	0.50	−36.9	−31.6
CHTD-D		D	0.25	−36.9	Not tested[e]
CHTD-E		E	1.00[f]	−37.4	−30.7

[a]Curing time 20 days for batches A–D, 3 days for batch E.
[b]HyTemp mass = 3.50 g.
[c]Measured at the inflection point.
[d]Measured at the maximum of the tanδ peak.
[e]Traces recovered after evaporating solvent from Soxhlet washings.
[f]With 2% w/w of ScTFMS accelerator.
[g]Evidence of a weak second transition.

(for example Sample CHTP-A, Figure 1) by ^{1}H NMR, by treating small aliquots (0.01 g mL^{-1}) from each cured mixture with acetone-d_6 or $CDCl_3$ for 1 h at room temperature to remove any excess of unreacted polymer and cross-linker. When short cross-linkers (EGDGE, TEGDGE, and DEO) were used, the relative curing mixtures (Samples CHTE, CHTT, and CHTD, Batches A–D) became insoluble in d-solvents after 3–4 days at 70°C. The conversion of the mixtures from viscous liquid to a gel (gelation point) matched with the beginning of the formation of the 3D cross-liked structure.[40] Longer gelation times, up to 7 days, were observed instead in samples CHTH and CHTP (Batches A–D) prepared using the longer cross-linkers HEGDGE and PEGDGE, respectively (Table 1). The progress of the curing was confirmed by the reduced amount of the unreacted reagents—soluble fraction in the deuterated solvent—and the consistency of the insoluble fractions (more firm gels) in the same solvent. In samples CHTH and CHTP a slowing of cross-linker consumption was seen after gelation on day 7, in comparison with those cured with CHTE, CHTT, and CHTD; this difference was attributed to the chain length of the cross-linker and the diluted pending glycidyl groups in the gel structure after one of the two glycidyl groups has reacted. The opposite effect has been observed when alkyldiamine cross-linkers were used for the synthesis of poly(*N*-isopropylacrylamide) (PNIPAAm) gels.[41]

All the samples from batches A–D were left in the oven for a total of 20 days until the consumption of cross-linker was completed/unchanged by ^{1}H NMR, the samples were then purified by hot extraction with acetone (Soxhlet). The soluble residues from the extraction contained traces of unreacted polymer and cross-linker; the relative highest absorptions of unreacted cross-linker were observed in ^{1}H NMR spectra of samples CHTE-A (Figure S6) CHTT-A, CHTH-A, and CHTP-A in accordance with the high HyTemp:cross-linker ratio used (3.50:1.00 w/w). The separation of the two components in the soluble fractions was not possible because of the small amounts recovered. Vice versa, ^{1}H NMR spectra of samples from Batches B, C, and D confirmed that the tiny amounts of extracts after purification were mainly made of unreacted polymer. Figure 2 reports ^{1}H NMR spectra of the soluble fractions in acetone-d_6 from CHTE samples after purification (Peaks at 3.95–4.20 ppm are assigned to methylene protons of polymeric pendant groups $COOCH_2(CH_2)_nCH_3$), 3.90–3.95 ppm assigned to methyl protons of polymeric pendant groups CH_3COO, 3.40–3.85 ppm assigned to methylene protons of cross-linker groups OCH_2CH_2O and 3.20 ppm assigned to methine protons of the two cross-linker rings CH-O.[42] The final products (transparent gels of different consistency depending on the length of the cross-linker) were dried and characterized by DSC, MDSC, DMA, and SEM.

All the samples from Batch E (CHTE-E, CHTT-E, CHTH-E, CHTP-E, and CHTD-E) made in presence of the curing accelerator ScTFMS (2% w/w) exhibited a rubbery yellow-orange texture after 1 day of curing. Additional curing experiments of HyTemp 4454, cured with the PEGDGE cross-linker and a variable content of the

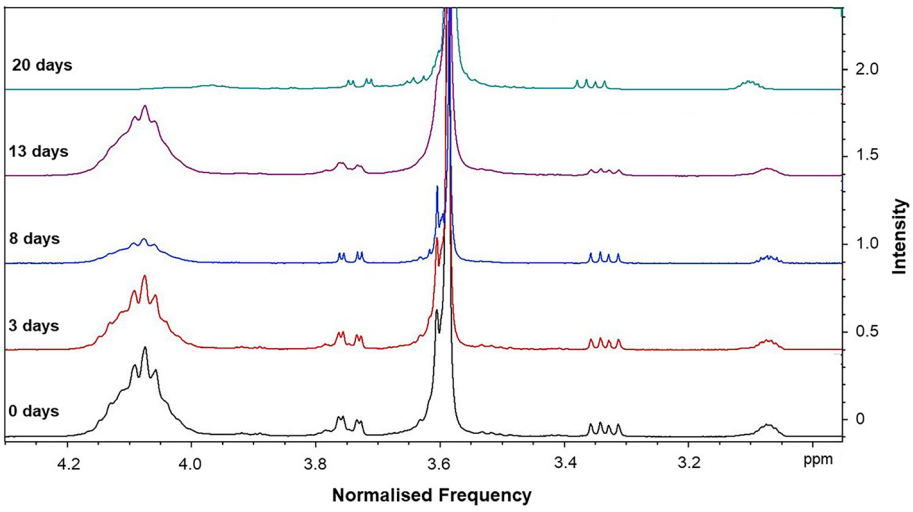

FIGURE 1 ^{1}H NMR curing monitoring of CHTP-A mixtures in acetone-d_6 (expanded area from 4.2 to 3.9 ppm) at (i) 0 days (black line, all soluble), (ii) 3 days (red line, all soluble), (iii) 8 days (blue line, only soluble fraction), (iv) 13 days (purple line, only soluble fraction), and (v) 20 days (green line, only soluble fraction, traces of cross-linker). The broad multiplet signal centrered at 4.05 ppm is attributed to HyTemp pendant methylene protons CH_2-OOC, the small broad peak at 3.80–3.75 ppm is assigned to HyTemp pendant methyl protons CH_3COO, the signals at 3.30–3.75 ppm are assigned to the methylene cross-linker protons OCH_2CH_2O while the multiplet signal centered at 3.07 ppm is assigned to the methine protons CH-O ring of the cross-linker[42] (Full spectra in SI).

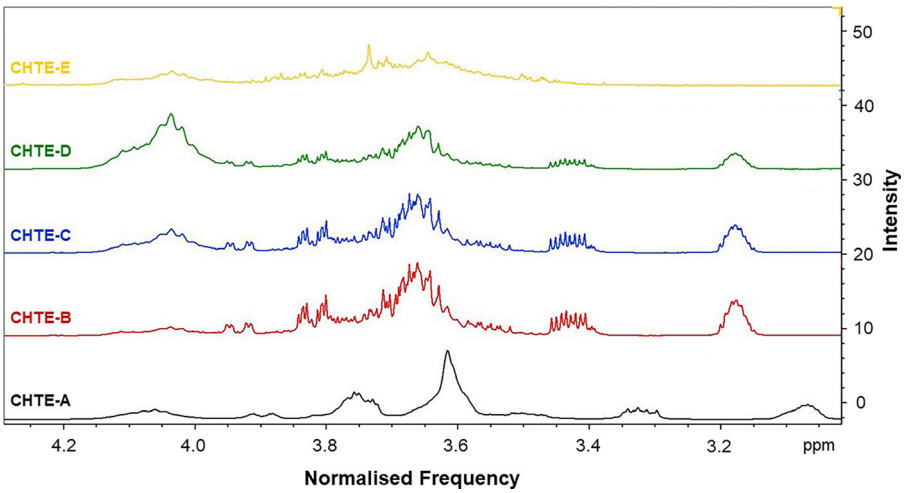

FIGURE 2 ^{1}H NMR spectra (from 4.3 to 2.9 ppm) of soluble fractions from purification of CHTE samples from batches A to E after 20 days of curing in acetone-d_6. (i) CHTE-A (black line, soluble fraction from Soxhlet extraction), (ii) CHTE-B (red line, soluble fraction from Soxhlet extraction), (iii) CHTE-C (blue line, soluble fraction from Soxhlet extraction), (iv) CHTE-D (green line, soluble fraction from Soxhlet extraction), and (v) CHTE-E (yellow line, soluble fraction of cured sample showing traces of unreacted).

accelerator (0.05%, 0.2%, and 0.5% w/w of the total mass of the polymer and cross-linker) confirmed curing times between 5 and 10 days. The color of the samples became more vivid with increasing concentrations of ScTFMS (Figure S7) suggesting that the samples retained some or all the salt used. However, a separate paper noted that the HyTemp 4454 resins cured with or without triflate catalyst, turned golden after curing.[13] The samples from Batch E were not purified by hot extraction from acetone as no residual cross-linker was detected by ^{1}H NMR in the soluble fraction after 1 day of curing (Figure 2). They were left in the oven for a total of 3 days and then dried and characterized by DSC.

Swelling experiments in ethyl acetate (2 h, ambient conditions) of all cured samples (Batches A–E) proved their ability to absorb the solvent and their volume increased with decreasing amount of cross-linker (Figure 3). Samples from Batch A absorbed more solvent resulting to a high percentage of swelling compared to all other samples from Batches B, C, and D (Table SWE -1, SI). The swelling degree of the samples significantly dropped in Batch E samples due to the high degree of cross-linking and the very compact 3D structures of these samples (CHTE-E, CHTT-E, CHTH-E, CHTP-E, and CHTD-E). The random distribution of the curable OH sites (pendant$_{COOH}$ and end groups$_{OH}$) in the HyTemp sample and the diffusion of the cross-linker molecules during curing in absence of solvent have affected the topology of the cross-linked microstructure of the cured samples,[43,44] and consequently the trend on the average swelling degree in all samples but not in CHTD (Figure 3). More investigation would be worth here for better understanding the influence of the number of ethylene glycol units (odd or even), presence of oxygen or other atoms in the cross-linker and folding of the cross-linker molecules (long or short) could influence the structure of the final 3D structures.

3.1 | Thermal characterization of cured samples

One of the main objectives of this research was to evaluate the glass transition of the cured samples, a second-order transition (with no heat transfer)[45] in which a polymer in a rubbery state on cooling changes to glassy state, or vice versa; this was determined by using DSC, both conventional and modulated, and by DMA. In all the thermograms recorded between −100 and 25°C, the only distinguishable feature found by DSC was the glass transition, apart from a few small artifacts, possibly due to impurities or instrument noise. Table 1 reports the T_g observed for the cured HyTemp samples prepared using different cross-linkers and HyTemp:cross-linker ratios (Batches A–D); for these samples there appears to be no significant difference between them, with all the T_gs being similar to pure HyTemp (−37.2°C).[38,45]

This is exemplified in Figure 4 for cured samples CHTE-A (black line), CHTT-A (red line), CHTH-A (blue line), CHTP-A (green line), and CHTD-A (yellow-orange line) made with the same ratio HyTemp:cross-linker (3.50:1.00), and Figure 5 (Top) for cured samples CHTE-A (black line), CHTE-B (red line), CHTE-C (blue line), and CHTE-D (green line) made with the same cross-linker (EGDGE) but variable amounts. Typically, the introduction of a cross-linker to a polymer result in an increase in the T_g due to a decrease in the mobility of the polymer, hence leading to a decrease in free volume.[46] Vice versa, the incorporation of a flexible spacer (comonomer) in an amorphous material increases the molecular mobility and decreases the T_g.[47] The hypothesis here is that the two cooperative effects with the synergy of the relatively low cross-linking degree maintained the T_g of the synthesized elastomers similar to the value of the starting polyacrylate.

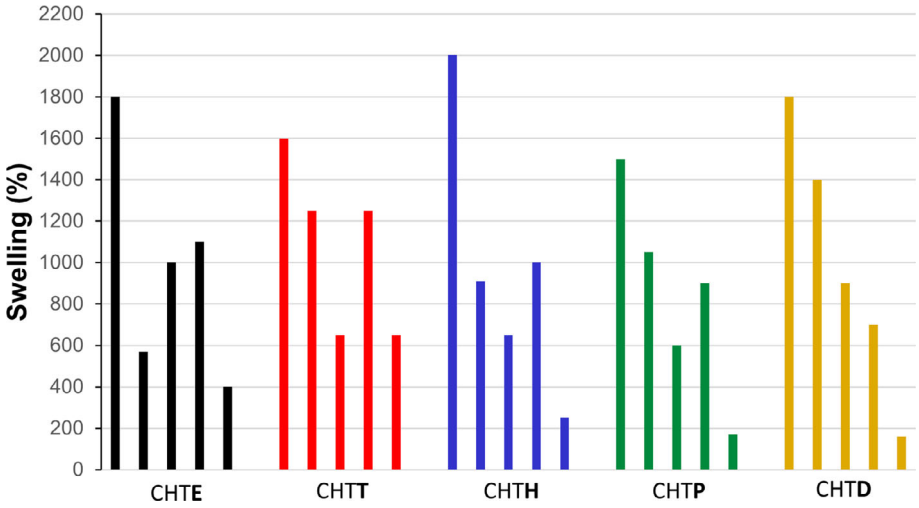

FIGURE 3 Swelling comparison of cured HyTemp samples CHTE, CHTT, CHTH, CHTP, and CHTD in ethyl acetate. Batches A to E from left to right.

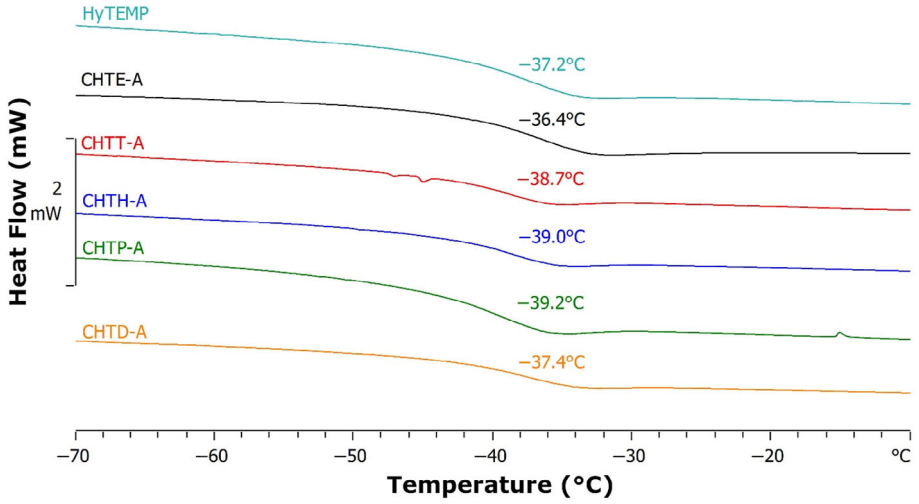

FIGURE 4 DSC thermogram for pristine HyTemp (light blue line) and cured samples CHTE-A (black line), CHTT-A (red line), CHTH-A (blue line), CHTP-A (green line), and CHTD-A (yellow-orange line) made with the same ratio HyTemp/cross-linker (3.50:1.00). From 2nd heating at 10°C.

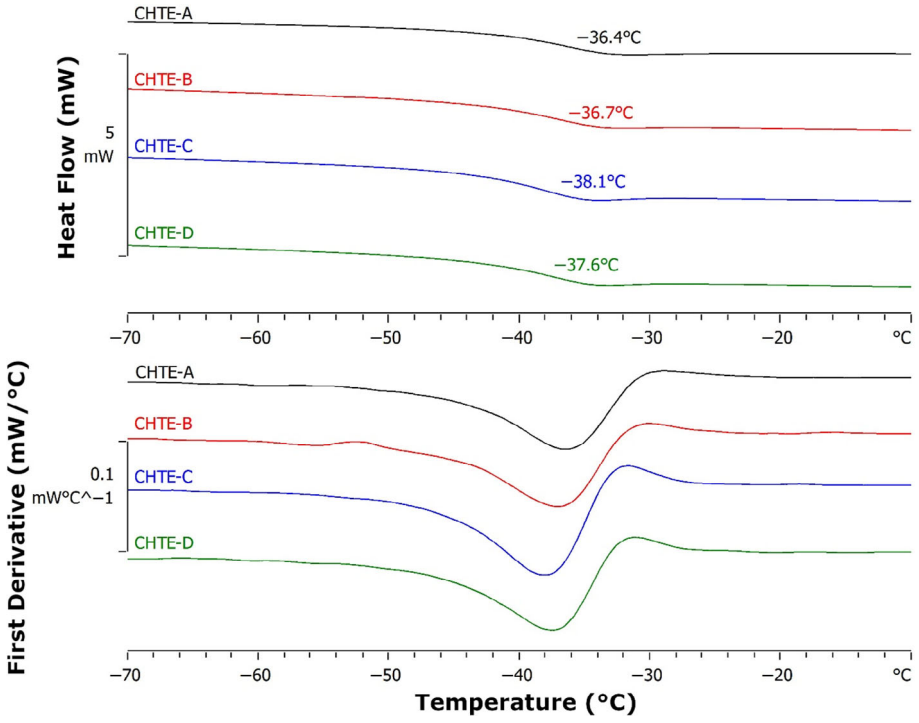

FIGURE 5 Top—DSC thermogram of HyTemp cured with differing amounts of EGDGE cross-linker (Samples CHTE-A, CHTE-B, CHTE-C, and CHTE-D). Bottom—First derivative of DSC curves shown above. DSC thermograms for samples CHTT, CHTH, CHTP, and CHTD are reported in Figures S8–S11.

The introduction of ScTFMS, as curing accelerator had an important effect on the glass transition of the samples in Batch E, as seen in Figure 6, Top. Samples CHTE-E, CHTT-E, CHTH-E, and CHTP-E appeared to have two glass transitions, shown by two steps. This was more evident when taking the first derivative of the DSC curve (Figure 6, bottom), which contained two inverted peaks on the curves. Looking closely at the first derivative for sample CHTT-E, there also appears to be two T_gs, at −39.2 and∼−32.0°C (although a precise value could not be calculated using the software). An example of the first derivatives of the DSC scan for samples CHTE-A, CHTE-B, CHTE-C, and CHTE-D (Figure 5, bottom) are shown for reference, showing only the single peak. This appears to be a kinetic effect, with the introduction of an accelerator causing regions of the polymer to be cross-linked in a different manner, hence a different T_g. Polymers with two glass transitions have been seen in block copolymers, for instance SEBS (Styrene-ethylene/butylene-styrene), with each block having a separate glass transition.[48] An additional glass transition has been previously seen with polymer composites with nanometric particles and in polyurea networks.[49,50] There are no other reports of addition of an accelerator causing dual glass transitions. Interestingly, the length of the cross-linker appears to influence the temperature of the additional T_g which can be explained by the presence of both end and side curable groups in HyTemp.[27,28] With the shortest cross-linker (Sample CHTE-E), the additional T_g is at −10.8°C, then sharply decreases to −30°C for sample CHTT-E, 45.2°C for sample CHTH-E, and finally at −47.4°C for sample CHTP-E. This decrease in the additional T_g with increasing length of cross-linker, was associated to the increased mobility of the longer cross-linker. The cooperative effect kept the T_g remarkably like the pristine HyTemp in samples from Batches A to D but in batch E the faster cross-linking appears to create a two-domain structure with a second T_g.

Further analysis of samples CHTE-E, CHTT-E, CHTH-E, CHTP-E, and CHTD-E was performed using Mettler Toledo's TOPEM multi-frequency modulated DSC. An example thermogram for CHTP-E is shown in Figure 7. Modulated DSC provides the user with additional information, for instance heat flow can be split into reversing and non-reversing components. A pure glass transition should be completely reversing; however, a glass transition is often accompanied by an enthalpic relaxation,[51] which would be non-reversing. As sample CHTP-E appears to have two glass transitions (two steps in the reversing curve), it also has two enthalpic relaxations (shown by two inverted peaks in the non-reversing curve). As TOPEM is a multi-frequency technique, the effect of frequency on the glass transition can also be assessed. Figure 7 bottom shows the effect of frequency on the storage heat capacity, this example clearly shows a strong frequency dependency with the transition, which is consistent with a glass transition.[52]

DMA measurements confirmed that the type and amount of cross-linker in samples in Batches A–C had no effect on the material's viscoelastic properties and glass

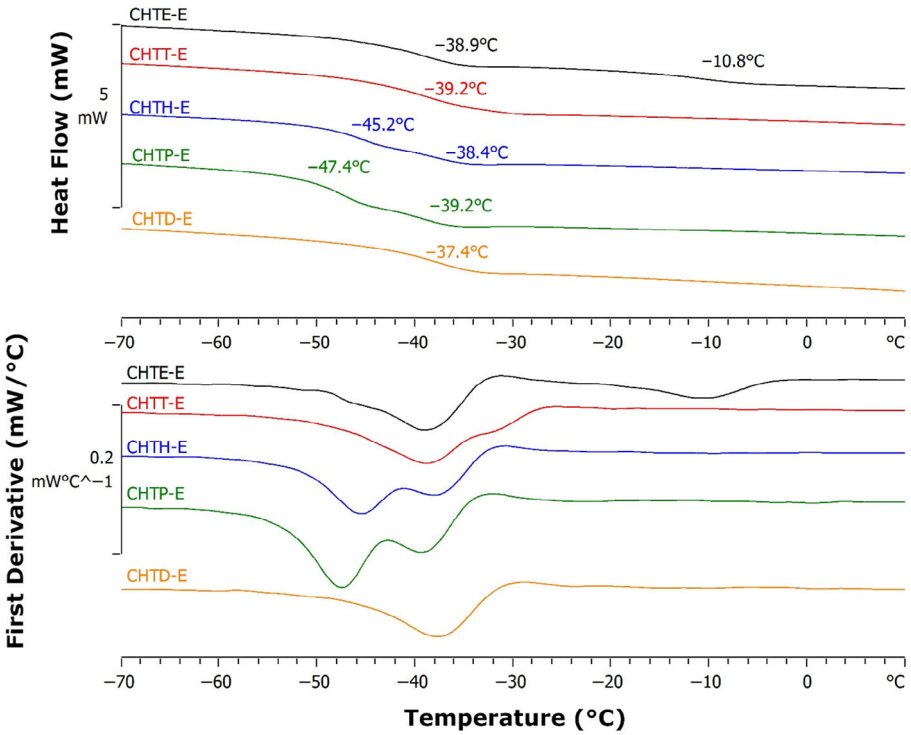

FIGURE 6 Top—DSC thermogram of cured samples CHTE-E, CHTT-E, CHTH-E, CHTP-E, and CHTD-E made using with different cross-linkers. Bottom—First derivative of DSC thermograms shown above.

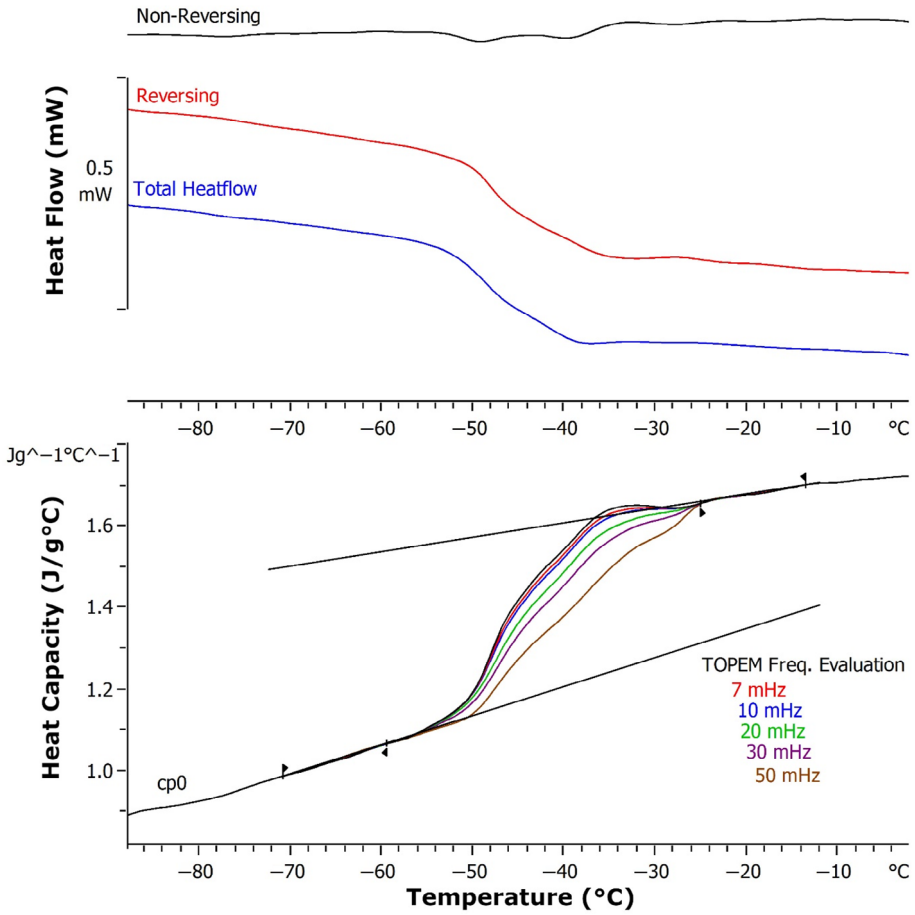

FIGURE 7 Top—Modulated (TOPEM) DSC for sample CHTP-E, showing the total flow (Blue line), reversing (Red line) and non-reversing (Black line) thermal profiles. Bottom—Heat capacity (cp0) dependency from frequency, at 7 mHz (Red line), 10 mHz (Blue line), 20 mHz (Green line), 30 mHz (Purple line) and 50 mHz (Brown line). MDSC thermograms for samples CHTE-E, CHTT-E, CHTH-E, and CHTD-E are reported in Figures S12–S15.

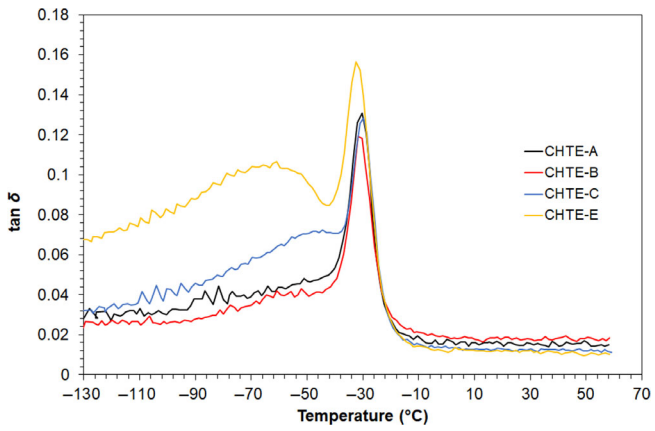

FIGURE 8 Tan δ curves for samples CHTE-A (black line), CHTE-B (red line), CHTE-C (blue line), and CHTE-E (yellow line). DMA thermograms for samples CHTT, CHTH, CHTP, and CHTD are reported in Figures S16–S19.

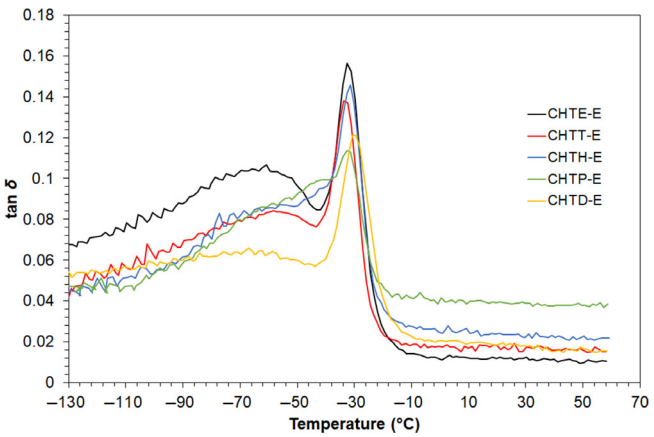

FIGURE 9 Tan δ curves for samples CHTE-E (black line), CHTT-E (red line), CHTH-E (blue line), CHTP-E (green line), and CHTD-E (yellow line).

transition temperatures (Table 1, Figure 8 for CHTE samples). The compositions of samples CHTE-D, CHTT-D, CHTH-D, CHTP-D, and CHTD-D were not analyzed by DMA due to traces recovered after evaporation of the solvent from Soxhlet washings. The values of the glass transition temperature from the tan δ peak remained constant at an average of -31.3 ± 0.8°C—similar value to the T_g of pure HyTemp (Table 1). On the other hand, the T_g temperature of Batch E samples (i.e., CHTE-E, CHTT-E, CHTH-C, CHTP-E, and CHTD-E) was slightly lower at an average of -33.0 ± 1.4°C compared with the other Batches A–D due to the use of the accelerator

(Figure 9). The second glass transition at lower temperature observed by DSC in samples CHTE-E, CHTT-E, CHTH-C, and CHTP-E was not visible in the DMA curves because it was hidden by the hump before the main tan δ peak between −70 and −60°C. This hump is associated to a rearrangement of the molecules resulting in the relief of stresses frozen in the compositions by the processing method.[53]

SEM micrographs gave an insight into the relationship between the structure and the properties of selected synthesized samples (CHTE-B, CHTE-E, CHTH-E, CHTP-B, and CHTP-E) and confirmed the modification of the bulk structure of HyTemp after cross-linking with the various cross-linkers in accordance with the design expectations.[54,55] The samples were examined before and after swelling in distilled water for 48 h at ambient temperature. There is a correlation between the length (EGDGE, HEGDGE and PEGDGE) and amount of cross-linker (3.5:1 w/w and 3.5:0.75 w/w), the speed of the cross-linking process (with (Batch E) or without (Batches A–D) curing accelerator) the size of the pores captured in the swelled samples (Table 2 and Figure 10).[56] Sample CHTE-E which cured quickly with the aid of the accelerator and with the shortest cross-linker (EGDGE) was characterized by higher porosity but smaller pore dimensions (1.13 nm) after swelling (Figure S20, left) compared with sample CHTE-B (1.56 nm) (Figure S20, middle) that

TABLE 2 Pore sizes of cured HyTemp samples before and after swelling in water for 48 Hours at ambient temperature (obtained from SEM images using ImageJ software).

Sample ID	Before swelling Pore dimensions (nm)[a]	After swelling
HyTemp	N/A	N/A
CHTE-E	0.29 ± 0.13	1.13 ± 0.18
CHTE-B	0.45 ± 0.03	1.56 ± 0.41
CHTH-E	1.25 ± 0.21	2.76 ± 0.12
CHTP-B	1.04 ± 0.21	4.92 ± 0.98
CHTP-E	1.57 ± 0.34	5.48 ± 1.24

[a]Average of three samples.

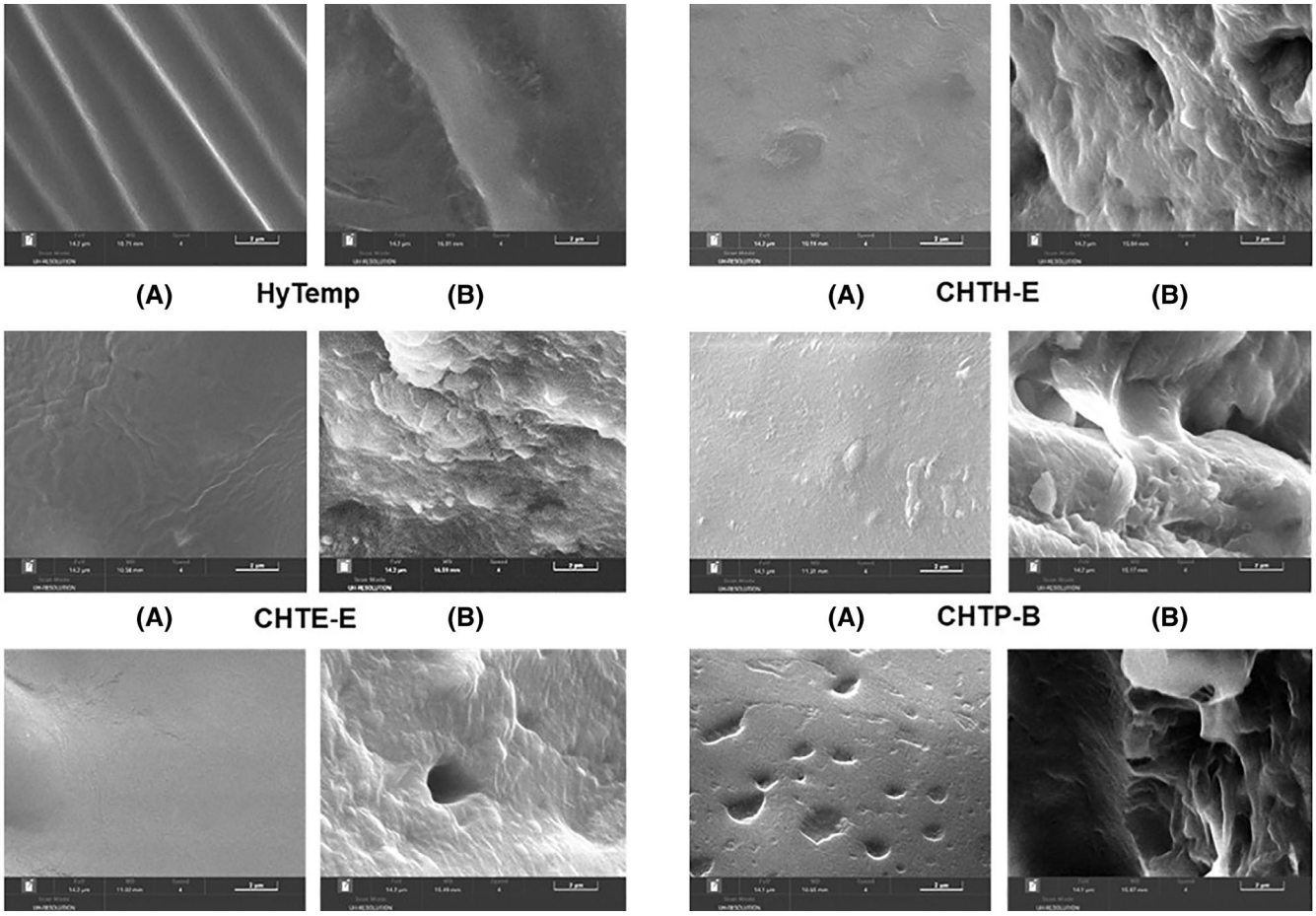

FIGURE 10 Scanning electron micrographs of crosslinked HyTemp (top left), CHTE-E (middle left), CHTE-B (bottom left), CHTH-E (top right), CHTP-B (middle right), and CHTP-E (bottom right) samples: (a) after cutting from freeze-drying and (b) after swelling in water (48 h) and cutting from freeze-drying showing the interior morphology at magnification 20 k.

was cured through a slower process without accelerator and the same cross-linker. Sample CHTH-E made from fast curing and a longer cross-linker (HEGDGE) exhibited a higher porosity density (Figure S20, right) and pore dimensions (2.76 nm) than the CHTE-E and CHTE-B samples. In samples CHTP-B and CHTP-E, the porosity was difficult to estimate due to pores being as not well-defined as in the CHTH samples; their pores (dimensions of 4.92 and 5.48 nm, respectively) were larger compared with all the other swelled samples examined by SEM. This analysis showed that the longer the cross-linker (Samples CHTH and CHTP) the larger the pore size when the elastomers were synthesized with or without accelerator. No pores were detected in HyTemp samples under the same experimental conditions (Figure 10 and Figure S21). The influence of the speed of the cross-linking process on the pore size became negligeable as the cross-linker length increased.

4 | CONCLUSIONS

The effect of the cross-linker length related to the number of ethylene glycol units and amount as well as the presence of a cross-linking accelerator on the curing of hydroxyl-terminated polyacrylic ester (HyTemp) was explored. It was found that after 20 days at 70°C, the novel 3D structures exhibited a remarkable increase in pore size captured by SEM with increasing cross-linker length and swelling ability. A kinetic effect induced by the curing accelerator ScTFMS caused two-domain structures in the polymeric samples with a dual T_g. For the first time, processing of the MDSC curves offered the possibility to capture structural differences in complex polymeric 3D structures. The new materials exhibit a potentially wider operational range due to an additional lower glass transition and high absorptivity opening the doors for designing a new class of micropore polymeric systems for the potential recovery of pollutants in soil and/or water.

ACKNOWLEDGMENTS

The authors would like to thank Dr. Nathan Flood from HSE UK, for his initial input on the use of MDSC for the characterization of the materials and Dr. Jonathan Painter from Cranfield University for some preliminary SEM consultancy and Mrs. Clare Pratchett for the input on the graphical abstract.

FUNDING INFORMATION

This research was funded by Cranfield University via a MSc project.

CONFLICT OF INTEREST STATEMENT

The authors declare no conflict of interest.

DATA AVAILABILITY STATEMENT

Data supporting this study are included within the article and/or supporting materials.

ORCID

Eleftheria Dossi https://orcid.org/0000-0001-6365-8019
Peter Wilkinson https://orcid.org/0000-0002-8028-3324
Guillaume Kister https://orcid.org/0000-0001-9763-0233
Hugh Patrick https://orcid.org/0009-0006-2177-9094
Mohammad Hakim Khalili https://orcid.org/0000-0001-6185-6716

REFERENCES

[1] K. Matyjaszewski, *Prog. Polym. Sci.* **2005**, *30*, 858.
[2] P. Mondal, P. K. Behera, N. K. Singha, *Prog. Polym. Sci.* **2021**, *113*, 101343.
[3] A. M. Gandini, T. Lacerda, *Molecules* **2022**, *27*, 159.
[4] J. P. Coats, R. Cochereau, I. A. Dinu, D. Messmer, F. Sciortino, C. G. Palivan, *Macromol. Biosci.* **2023**, *23*, 220047.
[5] E. Dossi, J. Earnshaw, L. Ellison, G. Rabello dos Santos, H. Cavaye, D. Cleaver, *Polym. Chem.* **2021**, *12*, 2606.
[6] M. H. Khalili, C. J. Williams, C. Micallef, F. Duarte-Martinez, A. Afsar, R. Zhang, S. Wilson, E. Dossi, S. A. Impey, S. Goel, A. I. Aria, *ACS Appl Polym Mater* **2023**, *5*, 1180.
[7] V. L. Popov, *Viscoelastic Properties of Elastomers, in: Contact Mechanics and Friction*, Springer-Verlag, Berlin Heidelberg **2010**, p. 231. https://doi.org/10.1007/978-3-642-10803-7
[8] L. M. Polgar, R. R. J. Cerpentier, G. H. Vermeij, F. Picchioni, M. van Duin, *Pure Appl. Chem.* **2016**, *88*, 1103.
[9] J. Kruželák, A. Kvasničáková, I. Hudec, *Adv. Ind. Eng. Polym. Res.* **2020**, *3*, 120.
[10] T. Oyama, in *Encyclopedia of Polymeric Nanomaterials* (Eds: S. Kobayashi, K. Müllen), Berlin, Heidelberg, Springer **2014**. https://doi.org/10.1007/978-3-642-36199-9_181-1
[11] E. Broughton, *Environ. Health* **2005**, *4*, 6.
[12] A. V. Cunliffe, D. A. Tod, S. A. Torry, *EP 2 283 061 B1*, QinetiQ Limited GB. **2011**.
[13] E. Dossi, J. Akhavan, R. G. Williams, W. J. Doe, S. Gaulter, *Propellants, Explos., Pyrotech.* **2018**, *43*, 241.
[14] J. Shen, X. Lin, J. Liu, X. Li, *Macromolecules* **2019**, *52*, 121.
[15] S. Heyden, R. W. Style, E. R. Dufresne, *Soft Matter* **2023**, *19*, 4385.
[16] N. Guarrotxena, I. Quijada-Garrido, *Chem. Mater.* **2016**, *28*, 1402.
[17] S. Khan, N. M. Ranjha, *Polym. Bull.* **2014**, *71*, 2133.
[18] S. Sonawane, M. Anniyappan, J. Athar, A. Singh, M. B. Talawar, R. K. Sinha, S. Banerjee, A. K. Sikder, *Propellants, Explos., Pyrotech.* **2017**, *42*, 386.
[19] K. Dusek, W. J. MacKnigh, *ACS Symposium Series*, American Chemical Society, Washington, DC **1988**. https://doi.org/10.1021/bk-1988-0367.ch001
[20] X. Teng, H. Xu, W. Song, J. Shi, J. Xin, W. C. Hiscox, J. Zhang, *ACS Omega* **2017**, *2*, 251.

[21] Y. Yang, H. Zhao, *Appl. Surf. Sci.* **2022**, *577*, 151895.
[22] M. A. Hussein, H. K. Albeladi, A. N. Al-Romaizan, *Int. J. Biosens. Bioelectron.* **2017**, *3*, 279.
[23] M. A. Hussein, R. M. El-Shishtawy, B. M. Abu-Zied, A. M. Asiri, *J. Therm. Anal. Calorim.* **2016**, *124*, 709.
[24] J. R. Choi, K. W. Yong, J. Y. Choi, A. C. Cowie, *BioTechniques* **2019**, *66*, 40.
[25] M. H. Khalili, V. Panchal, A. Dulebo, S. Hawi, R. Zhang, S. Wilson, E. Dossi, S. Impey, S. Goel, A. Aria, *ACS Appl. Polym. Mater.* **2023**, *5*, 3034.
[26] R. O. Moreno, E. K. Penott-Chang, B. Rojas de Gáscue, A. J. Müller, *Eur. Polym. J.* **2017**, *88*, 148.
[27] https://www.zeonchemicals.com/products/hytemp-acm/ (assessed: December 2023).
[28] M. T. M. Moutinho, B. F. Andrade, P. L. de Andrade Coutinho, *US 2005/0234207 A1*, 2005. Petroflex Industria E Comercio SA. **2005**.
[29] K. Venkataswamy, T. Abraham, *US6020431A*, 1998. ExxonMobil Chemical Co. **1998**.
[30] P. J. Hans, K. E. Jenkins, WO9110708 A1, *1991. General Electric Company* **1991**
[31] S. Habaue, H. Baraki, Y. Okamoto, *Polym. J.* **2000**, *32*, 1017.
[32] R. Horning, *US20190177528A1*, 2019. ElringKlinger AG. **2019**.
[33] https://www.zeon.eu/products/curatives-additives.html (assessed: April 2024).
[34] K. Venkataswamy, T. Abraham, *US6020431*, Advanced Elastomers Systems, L.P. **2000**.
[35] https://www.chemtechnologiesltd.com/media/1022/ctr-06001-advancuretm-low-cost-curative-for-vamac.pdf (assessed: April 2024).
[36] E. Dossi, From raw ingredients to energetic materials. in (Ed: A. S. Cumming), Energetics Science and Technology: An Integrated Approach, IOP, Bristol **2022**. https://doi.org/10.1088/978-0-7503-3943-8ch2
[37] R. J. Angelo, R. M. Ikeda, M. L. Wallach, *Polymer* **1965**, *6*, 141.
[38] https://msds-web.zeonchemicals.com/Access/Search.aspx?MHCHNM=HyTEmp%204454 (assessed: December 2023).
[39] F. Luppi, N. Mai, G. Kister, P. P. Gill, S. E. Gaulter, C. Stennett, E. Dossi, *Chem A European J* **2019**, *25*, 15646.
[40] C. J. Brinker, G. W. Scherer Eds., *Sol-Gel Science*, Academic Press, California **1990**, p. 302. https://doi.org/10.1016/B978-0-08-057103-4.50010-6
[41] S. Ida, A. Katsurada, M. Tsujio, M. Nakamura, Y. Hirokawa, *Gels* **2020**, *6*, 2.
[42] R. M. Silverstein, F. X. Webster, *Spectrometric Identification of Organic Compounds*, 6th ed., Wiley and Sons, Inc, United States **2003**.
[43] A. Klupplel, C. Mai, *Wood Sci. Technol.* **2013**, *47*, 643.
[44] D. Y. Kim, J. W. Park, D. Y. Lee, K. H. Seo, *Polymer* **2020**, *12*, 2020.
[45] J. H. Gibbs, E. A. DiMarzio, *J Chem Phys* **1958**, *28*, 373.
[46] C. C. Huang, M. X. Du, B. Q. Zhang, C. Y. Liu, *Macromolecules* **2022**, *55*, 3189.
[47] D. K. Schneiderman, M. A. Hillmyer, *Macromolecules* **2016**, *49*, 2419.
[48] C. A. Sierra, C. Galán, J. G. Fatou, M. D. Parellada, J. A. Barrio, *Polymer* **1997**, *38*, 4325.
[49] L. Li, D. Zhou, D. Huang, G. Xue, *Macromolecules* **2014**, *47*, 297.
[50] M. Reinecker, V. Soprunyuk, M. Fally, A. Sanchez-Ferrer, W. Schanz, *Soft Matter* **2014**, *10*, 5729.
[51] L. C. Thomas, *J. Chem. Inf. Model.* **2013**, *53*, 1689.
[52] L. C. Thomas, *TAinstruments.Co.Jp*. **2005**, 1–9. http://www.tainstruments.com/pdf/literature/TP007_MDSC_2_CalculationsandCalibrations.pdf (assessed: December 2023).
[53] K. P. Menard, *Dynamic Mechanical Analysis: A Practical Introduction*, CRC Press Taylor and Francis, Hoboken USA **2008**.
[54] X. Zhong, C. Ji, A. K. L. Chan, S. G. Kazarian, A. Ruys, F. Dehghani, *J. Mater. Sci.: Mater. Med.* **2011**, *22*, 279.
[55] F. Yan, J. Texter, in *Conference Proceedings of Smart Coatings*. Orlando, FL (Eds: T. Provder, J. Baghdachi), ACS Symposium Series; American Chemical Society, Washington **2009**, p. 72. https://doi.org/10.13140/2.1.5110.2404
[56] L. Zedler, X. Colom, J. Canavate, M. R. Saeb, J. T. Haponiuk, K. Formela, *Polymer* **2020**, *12*, 545.

SUPPORTING INFORMATION

Additional supporting information can be found online in the Supporting Information section at the end of this article.

How to cite this article: E. Dossi, K. L. Mutele-Nkuna, P. Wilkinson, G. Kister, H. Patrick, M. H. Khalili, S. Hawi, *J. Polym. Sci.* **2024**, 1. https://doi.org/10.1002/pol.20240152